

Theoretical Review of Rare B Decays

F. Mahmoudi

*Université de Lyon, Université Claude Bernard Lyon 1, CNRS/IN2P3,
Institut de Physique des 2 Infinis de Lyon, UMR 5822, F-69622, Villeurbanne, France and
Theoretical Physics Department, CERN, CH-1211 Geneva 23, Switzerland*

We present an overview of the recent neutral current B decays focusing on the deviations with respect to the Standard Model predictions that are observed in $b \rightarrow s\ell^+\ell^-$ transitions, and discuss their implications for new physics scenarios in a model-independent way by means of global statistical fits. The prospects for future discoveries in the individual channels, in particular using the theoretically clean observables are also addressed.

I. INTRODUCTION

Rare B decays are important probes for physics beyond the Standard Model (SM) as they are loop-suppressed in the SM and are therefore sensitive to new physics (NP) parameters. As sensitive flavour observables, they are connected to fundamental questions in particle physics and in particular play a key role in understanding the underlying pattern of the SM. Furthermore, they can provide guidance for NP model-building.

In the recent years, there have been several experimental measurements showing deviations with respect to the SM predictions, that are commonly referred to as flavour anomalies. The angular observable P'_5 of the $B \rightarrow K^*\mu^+\mu^-$ decay [1] was the first one measured by LHCb collaboration in 2013 [2] presenting more than 3σ discrepancy with the SM. Updated measurements by LHCb have persistently confirmed this tension, which can be explained with short distance new physics contributions to this decay [3, 4]. The overall $B \rightarrow K^*\mu^+\mu^-$ angular observables are in agreement (see e.g. [5]) and the tension is also supported by the recent angular analysis of $B^+ \rightarrow K^{*+}\mu^+\mu^-$ [6]. Another decay indicating tension with the SM is $B_s \rightarrow \phi\mu^+\mu^-$ [7–9], in particular its branching ratio is measured to be below SM prediction. This trend is observed in several other $b \rightarrow s\ell^+\ell^-$ branching ratios such as $B \rightarrow K\mu^+\mu^-$ [10] and $\Lambda_b \rightarrow \Lambda\mu^+\mu^-$ [11]. However, the branching ratios are dependent on the local form factors and suffer from large theoretical uncertainties [12–24]. The angular observables on the other hand, while having a reduced sensitivity to the form factor uncertainties [25, 26], receive still non-local contributions that are not fully under control in QCD factorisation [27]. Therefore, the significance of the deviations depend on the estimated size of the non-local effects. Recent theoretical progress has been achieved for a better control of these effects in Refs. [28–31].

Furthermore, a set of observables is defined in order to check lepton flavour universality violation (LFUV) in $b \rightarrow s\ell^+\ell^-$ decays as [32]

$$R_H = (B \rightarrow H\mu^+\mu^-)/(B \rightarrow He^+e^-), \quad (1)$$

with $H = K^+, K^*, \phi$, etc. Such ratios, contrary to the observables mentioned above, are very clean and precisely known in the SM (see Ref. [33] for a recent study of the QED corrections for these observables). Deviations from the SM predictions are seen in the LFUV ratios for R_K [34–36] and R_{K^*} [37] that are measured to be below the SM predictions. Similarly, the recent measurements of $R_{K_S^0}$ and $R_{K^{*+}}$ [38] although within 2σ of the SM predictions, show the same trend with the central values below the SM predictions.

Interestingly, modest signs of LFUV are also observed in flavour changing neutral current processes in the Kaon sector [39].

Another theoretically clean observable with an uncertainty of less than 5% is the branching ratio of $B_s \rightarrow \mu^+\mu^-$ which has been measured by several experiments. Here we consider the combination of ATLAS [40], CMS [41] and LHCb [42, 43] as given in Ref. [44].

While the significance of the reported anomalies taken individually is around $\sim 2 - 3\sigma$, when considered collectively they can find a common NP explanation with a much larger significance in a global analysis [44–49].

II. THEORETICAL SETUP AND UNCERTAINTIES

The description of $b \rightarrow s\ell^+\ell^-$ transitions is based on the effective Hamiltonian

$$\mathcal{H}_{\text{eff}} = -\frac{4G_F}{\sqrt{2}}V_{tb}V_{ts}^* \left\{ \sum_{i=1,\dots,6,8} C_i O_i + \sum_{i=7,9,10,Q_1,Q_2,T} (C_i O_i + C'_i O'_i) \right\}, \quad (2)$$

where G_F , V_{tb} and V_{ts} are the Fermi constant and two CKM matrix elements, respectively, and the O_i are local operators coming each with an associated Wilson coefficient C_i which is calculable perturbatively for a particular high-energy physics model.

The semileptonic part of the Hamiltonian (second term in the left hand side) accounts for the domi-

nant contribution and can be factorised into a leptonic and a hadronic piece. The latter can be described by seven independent form factors $\tilde{S}, \tilde{V}_\lambda, \tilde{T}_\lambda$, with helicities $\lambda = \pm 1, 0$. The hadronic part of the Hamiltonian (first term in the left hand side) has a subleading contribution to $B \rightarrow K^* \mu^+ \mu^-$ from a virtual photon decaying into a lepton pair. This leads to non-factorisable contributions and appears in the vectorial helicity amplitudes

$$H_V(\lambda) = -i N' \left\{ C_9^{\text{eff}} \tilde{V}_\lambda - C_9' \tilde{V}_{-\lambda} + \frac{m_B^2}{q^2} \left[\frac{2 \hat{m}_b}{m_B} (C_7^{\text{eff}} \tilde{T}_\lambda - C_7' \tilde{T}_{-\lambda}) - 16 \pi^2 \mathcal{N}_\lambda \right] \right\}, \quad (3)$$

where the factorisable piece is described as the effective part of $C_9^{\text{eff}} (\equiv C_9 + Y(q^2))$ and the non-factorisable piece is encoded in $\mathcal{N}_\lambda(q^2) \equiv \text{Leading order in QCDf} + h_\lambda(q^2)$, with h_λ denoting the unknown power corrections. The short-distance NP contributions due to C_9 (and/or C_7) can be mimicked by long-distance effects in h_λ . Hence, the estimation of the size of the hadronic contributions is crucial in determining whether the observed deviations are due to new physics.

It is possible to parameterise the power corrections by a polynomial with a number of free parameters to be fitted to the experimental data [50]. Assuming a q^2 -polynomial ansatz [51, 52] we can write

$$h_\pm(q^2) = h_\pm^{(0)} + \frac{q^2}{1 \text{ GeV}^2} h_\pm^{(1)} + \frac{q^4}{1 \text{ GeV}^4} h_\pm^{(2)}, \quad (4)$$

$$h_0(q^2) = \sqrt{q^2} \times \left(h_0^{(0)} + \frac{q^2}{1 \text{ GeV}^2} h_0^{(1)} + \frac{q^4}{1 \text{ GeV}^4} h_0^{(2)} \right),$$

which is the most general ansatz for the unknown hadronic contributions (up to higher order powers in q^2) compatible with the analyticity structure assumed in Ref. [28].

By doing separate fits for NP and hadronic parameters, a statistical comparison between the two fits is possible using the Wilks' theorem [53]. As was shown in Ref. [54], while NP explanation seems to be favoured, more data is needed to be able to make conclusive statements.

III. GLOBAL FITS

Global statistical fits of the Wilson coefficients with the available data are a standard way to search for evidence for NP contributions, in a way that is agnostic to the specific NP model.

In order to check the coherence of the implication of the clean observables for new physics compared to the rest of the observables, we first present a fit to the former where we consider $\text{BR}(B_{s,d} \rightarrow \mu^+ \mu^-)$, R_K, R_{K^*} as well as the recently measured $R_{K_S^0}$ and $R_{K^{*+}}$ [38].

TABLE I: Fit to clean observables with the full data from 2021.

Only LFUV ratios and $B_{s,d} \rightarrow \ell^+ \ell^-$ ($\chi_{\text{SM}}^2 = 34.25$, nr. obs. = 12)			
	b.f. value	χ_{min}^2	Pulls _{SM}
δC_9	-2.00 ± 5.00	34.1	0.4σ
δC_9^e	0.83 ± 0.21	14.5	4.4σ
δC_9^μ	-0.80 ± 0.21	15.4	4.3σ
δC_{10}	0.43 ± 0.24	30.6	1.9σ
δC_{10}^e	-0.81 ± 0.19	12.3	4.7σ
δC_{10}^μ	0.66 ± 0.15	10.3	4.9σ
δC_{LL}^e	0.43 ± 0.11	13.3	4.6σ
δC_{LL}^μ	-0.39 ± 0.08	10.1	4.9σ

The calculation of the observables and the χ^2 fitting is done with the SuperIso public program [55–59].

A. Clean observables

In Table I the one-dimensional NP fit to clean observables are provided. Compared to the NP fit to the clean observables in Ref. [44], the two recently measured LFUV ratios $R_{K_S^0}$ and $R_{K^{*+}}$ [38] as well as the R_K measurement by Belle [60] in the [1,6] GeV² bin are included in the fit. While the hierarchy of the most favoured scenarios has remained the same, the addition of the two former measurements has resulted in an increase in the NP significance compared to [44] ($\sim 0.4\sigma$ for NP in $C_{\text{LL}}^{e,\mu}$, $C_{10}^{e,\mu}$ and 0.3σ for $C_9^{e,\mu}$). The inclusion of $\text{BR}(B_s \rightarrow \mu^+ \mu^-)$ in this set of observables is crucial in breaking the degeneracy between NP in C_9^μ and C_{10}^μ for explaining the measured values of the ratios (see Fig. 1).

B. All observables except the clean ones

In Table II we give the one-dimensional NP fit to all observables except the LFUV ratios and $B_{s,d} \rightarrow \ell^+ \ell^-$. In this set, the significance of the NP fit is dependent on the assumption for the size of the non-factorisable power corrections. The results of Table II is given with the assumption of 10% power correction. Compared to Ref. [44], the previous LHCb results of the $B_s \rightarrow \phi \mu^+ \mu^-$ observables are replaced by the recent measurements with an integrated luminosity of 8.4 fb⁻¹ [8, 9]. We also include the $F_H(B^+ \rightarrow K^+ \mu^+ \mu^-)$ measurement by CMS [61] as well as the $B \rightarrow K^* e^+ e^-$ angular observable measurements by LHCb [62]. With

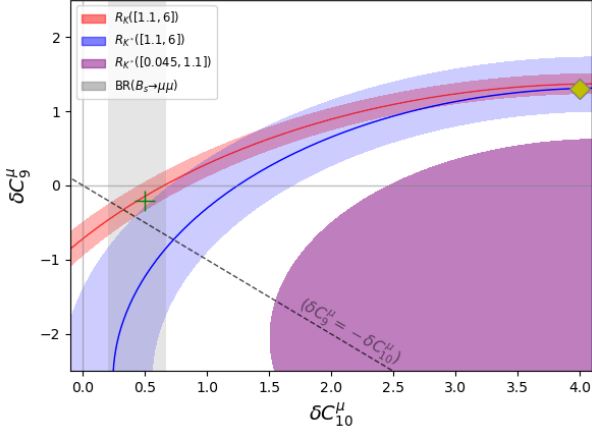


FIG. 1: The coloured and grey regions correspond to the values of δC_9^μ and δC_{10}^μ that result in a prediction of $R_{K^{(*)}}$ and $\text{BR}(B_s \rightarrow \mu^+ \mu^-)$ within 1σ ($= \sqrt{\sigma_{\text{th}}^2 + \sigma_{\text{exp}}^2}$) of their measured values, respectively. The solid red (blue) line corresponds to the LHCb measured central value for $R_{K^{(*)}}$ in the $q^2 \in [1.1, 6]$ GeV² bin. The yellow diamond (green cross) indicates the best fit value to $R_{K^{(*)}}$ excluding (including) $\text{BR}(B_s \rightarrow \mu^+ \mu^-)$. See caption of Fig. 3 in Ref. [44] for further information.

TABLE II: Fit to all except the clean observables with the full data from 2021.

All observables except LFUV ratios and $B_{s,d} \rightarrow \ell^+ \ell^-$ ($\chi_{\text{SM}}^2 = 221.8$, nr. obs.= 171)			
	b.f. value	χ_{min}^2	Pull _{SM}
δC_9	-0.95 ± 0.13	185.1	6.1σ
δC_9^e	0.70 ± 0.60	220.5	1.1σ
δC_9^μ	-0.96 ± 0.13	182.8	6.2σ
δC_{10}	0.29 ± 0.21	219.8	1.4σ
δC_{10}^e	-0.60 ± 0.50	220.6	1.1σ
δC_{10}^μ	0.35 ± 0.20	218.7	1.8σ
δC_{LL}^e	0.34 ± 0.29	220.6	1.1σ
δC_{LL}^μ	-0.64 ± 0.13	195.0	5.2σ

these updates, the hierarchy of the most favoured scenarios has remained the same, with the largest significance for NP in vector lepton current in the muon sector δC_9^μ or by lepton flavour universal NP in δC_9 followed by NP in the chiral basis δC_{LL}^μ in the muon sector. These three favoured scenarios are all now showing a reduction of $\sim 0.4\sigma$ compared to Ref. [44] which can be attributed mostly to the updated measurement of the $B_s \rightarrow \phi \mu^+ \mu^-$ observables.

The fit with all observables except the clean ones

shows no indication for NP in the electron sector, however, besides the agreement of the measurements in the electron sector with their SM predictions, it should be noted that in this set of observables the experimental data in the electron mode is much scarcer compared to the muon sector. Comparison of Tables I and II shows that there is not a complete consistency between all favoured scenarios for each of the two datasets. However, there are scenarios such as NP in δC_9^μ for which not only there is a large significance for both datasets but also the best fit values agree within 1σ .

C. Global fit to all $b \rightarrow s \ell^+ \ell^-$ observables

To get the global picture of the rare B -decays, we consider here all the relevant observables (consisting of the clean and the rest of the observables mentioned in the previous subsections). For the global fit, similar to the fits of subsection III B, we consider 10% uncertainty for the power corrections.

1. One-dimensional fit

In Table III the one-dimensional global fits of NP to all relevant rare B -decays are given. As expected, the scenario with highest significance corresponds to NP in δC_9^μ , this is followed by NP in δC_{LL}^μ and the lepton flavour universal contribution δC_9 . This pattern is similar to what was observed in Ref. [44], while now the significance has reduced very slightly ($\sim 0.1\sigma$) for δC_9^μ and δC_{LL}^μ and $\sim 0.4\sigma$ for δC_9 . In Table III we have not considered scenarios with NP contribution to the electromagnetic dipole coefficient C_7 or

TABLE III: Fit to all observables with the full data from 2021.

All observables ($\chi_{\text{SM}}^2 = 253.3$, nr. obs.= 183)			
	b.f. value	χ_{min}^2	Pull _{SM}
δC_9	-0.93 ± 0.13	218.4	5.9σ
δC_9^e	0.82 ± 0.19	232.3	4.6σ
δC_9^μ	-0.90 ± 0.11	197.7	7.5σ
δC_{10}	0.27 ± 0.17	250.5	1.7σ
δC_{10}^e	-0.78 ± 0.18	230.4	4.8σ
δC_{10}^μ	0.54 ± 0.12	231.5	4.7σ
δC_{LL}^e	0.42 ± 0.10	231.2	4.7σ
δC_{LL}^μ	-0.46 ± 0.07	208.2	6.7σ

the (pseudo)scalar coefficients ($C_{Q_{1,2}}$) since in a one-dimensional fit these get highly constrained, the former by $B \rightarrow X_s \gamma$ and the latter by $B_s \rightarrow \mu^+ \mu^-$. We have also not given NP fits to contribution to right-handed quark currents ($\delta C'_i$) which are not favoured by the data. However in general in a multidimensional fit the situation can change as for example pointed out for the pseudo(scalar) contributions which when varied together with C_{10} can admit a large range of values [54].

2. Multidimensional fit

In general, UV-complete new physics models can contribute to several Wilson coefficients in the Weak effective theory, it is thus reasonable to make a multidimensional fit where more than one Wilson coefficient can be varied. Table IV presents the result of a twenty-dimensional fit to the rare B decay observables when varying all Wilson coefficients. Within this approach we avoid any look elsewhere effect (LEE). In general, LEE gets introduced when concentrating on a subset of observables, it also takes place if one and/or two specific NP directions are assumed a posteriori. However, this is avoided when assuming all possible Wilson coefficients. In principle, there might be insensitive coefficients and flat directions leading to an underestimation of the significance of the multidimensional fit. However, by considering likelihood profiles and correlation matrices we eliminate these

TABLE IV: 20-dimensional fit to all observables with the full data from 2021.

All observables with $\chi^2_{\text{SM}} = 253.3$, nr. obs. = 183 ($\chi^2_{\text{min}} = 179.2$; Pull _{SM} = 5.5(5.5) σ)			
δC_7 0.06 ± 0.03		δC_8 -0.80 ± 0.40	
$\delta C'_7$ -0.01 ± 0.01		$\delta C'_8$ -0.30 ± 1.30	
δC_9^μ -1.15 ± 0.18	δC_9^e -6.60 ± 1.60	δC_{10}^μ 0.21 ± 0.20	δC_{10}^e 2.60 ± 2.7
$\delta C_9^{\prime\mu}$ 0.05 ± 0.31	$\delta C_9^{\prime e}$ 1.40 ± 2.10	$\delta C_{10}^{\prime\mu}$ -0.04 ± 0.19	$\delta C_{10}^{\prime e}$ 1.30 ± 2.8
$C_{Q_1}^\mu$ 0.07 ± 0.06	$C_{Q_1}^e$ -1.60 ± 1.60	$C_{Q_2}^\mu$ -0.11 ± 0.14	$C_{Q_2}^e$ -4.00 ± 1.2
$C_{Q_1}^{\prime\mu}$ -0.07 ± 0.06	$C_{Q_1}^{\prime e}$ -1.70 ± 1.30	$C_{Q_2}^{\prime\mu}$ -0.21 ± 0.15	$C_{Q_2}^{\prime e}$ -4.10 ± 0.8

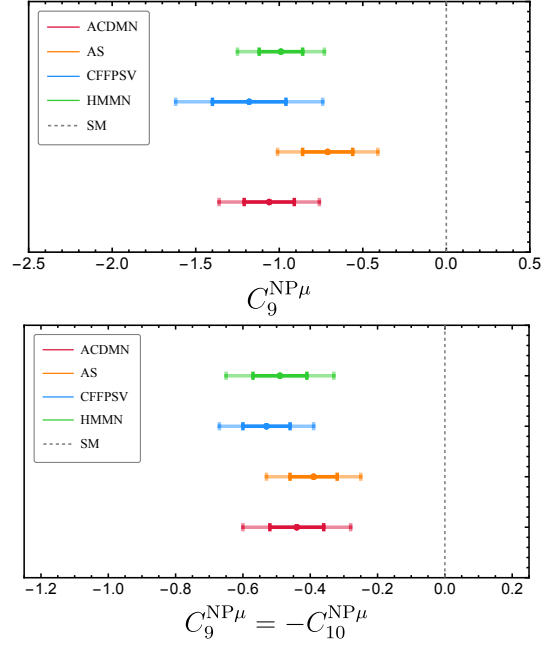


FIG. 2: Comparison of one-dimensional fits for NP contributions to C_9^μ (top) and to $C_9^\mu = -C_{10}^\mu$ (bottom). The darker (lighter) coloured lines correspond to 68% (95%) CL intervals. See the main text for the definition and the relevant reference for each group.

coefficients, finding an “effective” number of degrees of freedom (for the 20-dimensional fit we find 19 effective dof). The significance of the 20-dimensional fit is 5.5σ , similar to what was obtained in Ref. [44]. Several of the Wilson coefficients are still only loosely constrained as less data with electrons in the final state is available than with muons in the final state.

IV. COMPARISON OF GLOBAL FIT RESULTS

Here we present a comparison between global fits performed by the different fitting groups, based on the common work presented at the Flavour Anomaly Workshops [63, 64], where the results of the following groups have been confronted:

- ACDMN: M. Algueró, B. Capdevila, S. Descotes-Genon, J. Matias, M. Novoa-Brunet [45].
- AS: W. Altmannshofer, P. Stangl [46].
- CFFPSV: M. Ciuchini, M. Fedele, E. Franco, A. Paul, L. Silvestrini, M. Valli [47].
- HMMN: T. Hurth, F. Mahmoudi, D. Martínez-Santos, S. Neshatpour [44].

Similar fits have also been performed in [48, 65–68]. Fig. 2 shows the one-dimensional global fit results for C_9^μ and $C_9^\mu = -C_{10}^\mu$, and Fig. 3 shows the two-

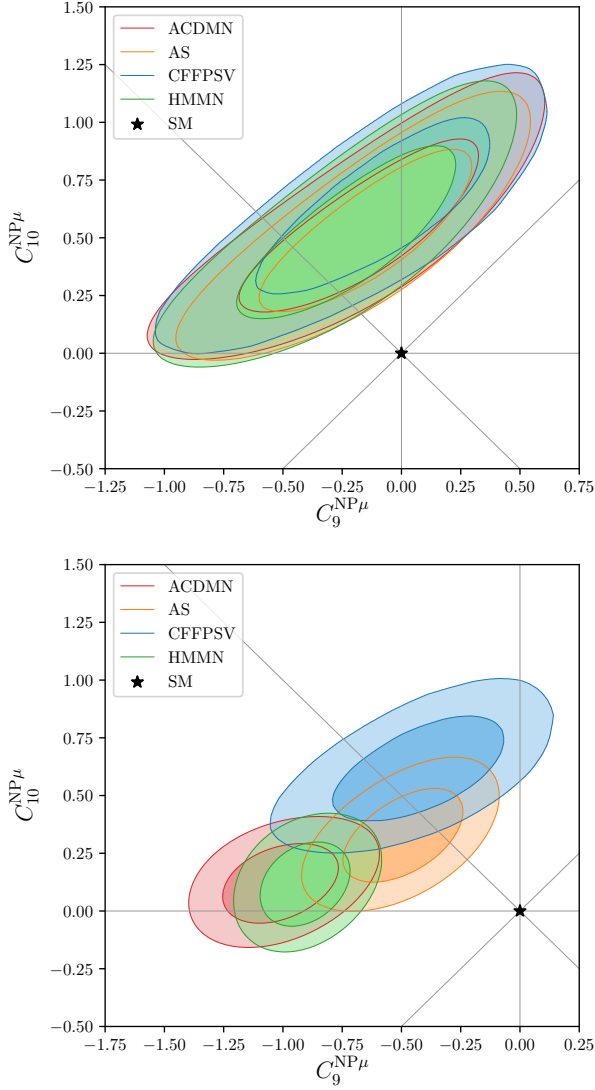


FIG. 3: Comparison of two-dimensional fits for NP contributions to $\{C_9^\mu, C_{10}^\mu\}$ using the clean observables (top) and using all available $b \rightarrow s\ell\ell$ data (bottom). The darker (lighter) coloured regions correspond to 68% (95%) CL fit results. See the main text for the definition and relevant reference for each group.

dimensional fits for clean observables (upper plot) and for all $bs\ell\ell$ observables (lower plot).

While there are differences in experimental inputs, form factors, assumptions on non-local matrix elements and statistical frameworks considered by different groups (see [63, 64] for more details), Figs. 2 and 3 show a remarkable global agreement between different results and the robustness of the conclusions.

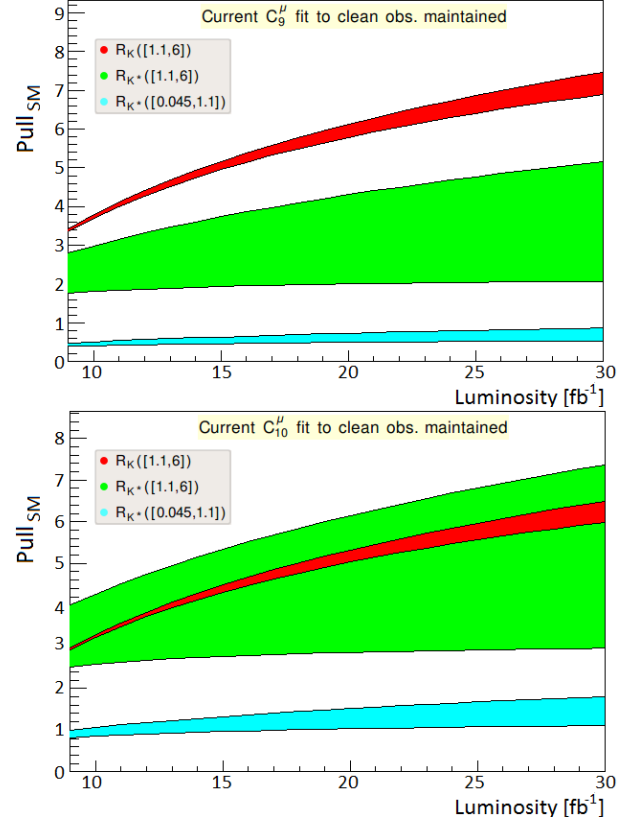


FIG. 4: Pull_{SM} for $R_K[1.1, 6]$, $R_{K^*}[1.1, 6]$ and $R_{K^*}[0.045, 1.1]$ as a function of LHCb integrated luminosity assuming the current best fit point for NP in C_9^μ (C_{10}^μ) for the top (bottom) plot.

V. PROJECTIONS FOR CLEAN OBSERVABLES

The global fit to rare B -decay observables suggests several NP scenarios with quite large significances. However, these significances are dependent on the assumed size of non-factorisable power corrections. It is thus useful to check when the clean observables (which are theoretically very precisely predicted) can individually reach a 5σ significance. In Fig. 4, assuming the current best fit value from the clean observables in the one-dimensional fit to δC_9^μ (δC_{10}^μ) remains, in the upper (lower) plot we have shown the significance of R_K and R_{K^*} as a function of the luminosity with the upper and lower bound for each observable corresponding to two different assumptions on the systematic uncertainties [69] (for further details see Ref. [44]). From Fig. 4 it is clear that if the current fit to δC_9^μ or to δC_{10}^μ is the correct description of new physics, R_K can reach 5σ already with less than 20 fb^{-1} of data.

We also make projections for the two-dimensional fits to all clean observables assuming the current best fit values for $\{C_9^e, C_9^\mu\}$ or $\{C_9^\mu, C_{10}^\mu\}$ remain. The results are given in Fig. 5 for the planned LHCb up-

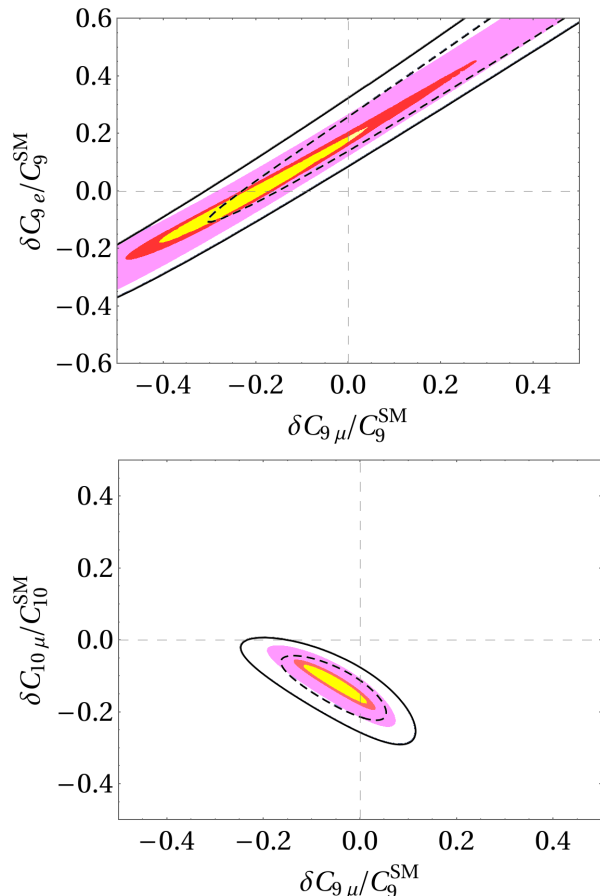


FIG. 5: Projection of the clean observables, assuming current $\{C_9^\mu, C_9^e\}$ ($\{C_9^\mu, C_{10}^\mu\}$) two-dimensional best fit point remains in the top (bottom) plot. The dashed and solid lines indicate the contour of the 68% and 95% CL fit with the current data, respectively. The pink, red and yellow regions correspond to 95% CL projections with 18, 50 and 300 fb^{-1} of data, respectively.

grades, for three benchmark points with 18, 50 and 300 fb^{-1} integrated luminosities. The best fit points for each scenario has a Pull_{SM} larger than 5σ already with 18 fb^{-1} data.

VI. CONCLUSIONS

The updated NP fits to rare B decays including the updated measurement of $B_s \rightarrow \phi \mu^+ \mu^-$ observables as well as the recent measurement of lepton flavour violating ratios $R_{K^{**}}$ and R_{K_S} by LHCb follow the same trend as with the previous set of results favouring in particular new physics contributions in the Wilson coefficient C_9^μ , with an increased significance. Interestingly, while the updated measurements have slightly changed the NP significance, the hierarchy of the preferred scenarios has remained the same. The projections for clean observables, show that if the current tensions remain, R_K can establish NP with 5σ significance already with less than 20 fb^{-1} of data. The main source of theory uncertainty in global fits is due to non-local hadronic contributions. However, different fits with different setups, inputs and statistical frameworks show a remarkable agreement so that the experimental observation of the discrepancy in these observables would be a clear sign of physics beyond the SM.

Acknowledgments

FM would like to thank the organisers of the FPCP 2022 conference for their invitation to present this talk, and for the very fruitful conference. She is also grateful to her collaborators and in particular to S. Neshatpour for his help in updating the fit results.

-
- [1] S. Descotes-Genon, J. Matias, M. Ramon, and J. Virto, *JHEP* **01**, 048 (2013), arXiv:1207.2753 [hep-ph].
 - [2] R. Aaij *et al.* (LHCb), *Phys. Rev. Lett.* **111**, 191801 (2013), arXiv:1308.1707 [hep-ex].
 - [3] R. Aaij *et al.* (LHCb), *JHEP* **02**, 104 (2016), arXiv:1512.04442 [hep-ex].
 - [4] R. Aaij *et al.* (LHCb), *Phys. Rev. Lett.* **125**, 011802 (2020), arXiv:2003.04831 [hep-ex].
 - [5] T. Hurth, F. Mahmoudi, and S. Neshatpour, *Phys. Rev. D* **103**, 095020 (2021), arXiv:2012.12207 [hep-ph].
 - [6] R. Aaij *et al.* (LHCb), *Phys. Rev. Lett.* **126**, 161802 (2021), arXiv:2012.13241 [hep-ex].
 - [7] R. Aaij *et al.* (LHCb), *JHEP* **09**, 179 (2015), arXiv:1506.08777 [hep-ex].
 - [8] R. Aaij *et al.* (LHCb), *JHEP* **11**, 043 (2021), arXiv:2107.13428 [hep-ex].
 - [9] R. Aaij *et al.* (LHCb), *Phys. Rev. Lett.* **127**, 151801 (2021), arXiv:2105.14007 [hep-ex].
 - [10] R. Aaij *et al.* (LHCb), *JHEP* **06**, 133 (2014), arXiv:1403.8044 [hep-ex].
 - [11] R. Aaij *et al.* (LHCb), *JHEP* **06**, 115 (2015), [Erratum: *JHEP* 09, 145 (2018)], arXiv:1503.07138 [hep-ex].
 - [12] A. G. Grozin and M. Neubert, *Phys. Rev. D* **55**, 272 (1997), arXiv:hep-ph/9607366.
 - [13] F. Kruger, L. M. Sehgal, N. Sinha, and R. Sinha, *Phys. Rev. D* **61**, 114028 (2000), arXiv:hep-ph/9907386.
 - [14] M. Beneke, T. Feldmann, and D. Seidel, *Nucl. Phys. B* **612**, 25 (2001), arXiv:hep-ph/0106067.

- [15] H. H. Asatryan, H. M. Asatrian, C. Greub, and M. Walker, *Phys. Rev. D* **65**, 074004 (2002), arXiv:hep-ph/0109140.
- [16] B. Grinstein and D. Pirjol, *Phys. Rev. D* **70**, 114005 (2004), arXiv:hep-ph/0404250.
- [17] M. Beneke, T. Feldmann, and D. Seidel, *Eur. Phys. J. C* **41**, 173 (2005), arXiv:hep-ph/0412400.
- [18] F. Kruger and J. Matias, *Phys. Rev. D* **71**, 094009 (2005), arXiv:hep-ph/0502060.
- [19] A. Khodjamirian, T. Mannel, A. A. Pivovarov, and Y. M. Wang, *JHEP* **09**, 089 (2010), arXiv:1006.4945 [hep-ph].
- [20] M. Beylich, G. Buchalla, and T. Feldmann, *Eur. Phys. J. C* **71**, 1635 (2011), arXiv:1101.5118 [hep-ph].
- [21] T. Nishikawa and K. Tanaka, *Nucl. Phys. B* **879**, 110 (2014), arXiv:1109.6786 [hep-ph].
- [22] A. Khodjamirian, T. Mannel, and Y. M. Wang, *JHEP* **02**, 010 (2013), arXiv:1211.0234 [hep-ph].
- [23] C. Hambroek, G. Hiller, S. Schacht, and R. Zwicky, *Phys. Rev. D* **89**, 074014 (2014), arXiv:1308.4379 [hep-ph].
- [24] J. Lyon and R. Zwicky, (2014), arXiv:1406.0566 [hep-ph].
- [25] U. Egede, T. Hurth, J. Matias, M. Ramon, and W. Reece, *JHEP* **11**, 032 (2008), arXiv:0807.2589 [hep-ph].
- [26] U. Egede, T. Hurth, J. Matias, M. Ramon, and W. Reece, *JHEP* **10**, 056 (2010), arXiv:1005.0571 [hep-ph].
- [27] T. Hurth, F. Mahmoudi, and S. Neshatpour, *Nucl. Phys. B* **909**, 737 (2016), arXiv:1603.00865 [hep-ph].
- [28] C. Bobeth, M. Chrzaszcz, D. van Dyk, and J. Virto, *Eur. Phys. J. C* **78**, 451 (2018), arXiv:1707.07305 [hep-ph].
- [29] V. M. Braun, Y. Ji, and A. N. Manashov, *JHEP* **05**, 022 (2017), arXiv:1703.02446 [hep-ph].
- [30] N. Gubernari, D. van Dyk, and J. Virto, *JHEP* **02**, 088 (2021), arXiv:2011.09813 [hep-ph].
- [31] N. Gubernari, M. Reboud, D. van Dyk, and J. Virto, (2022), arXiv:2206.03797 [hep-ph].
- [32] G. Hiller and F. Kruger, *Phys. Rev. D* **69**, 074020 (2004), arXiv:hep-ph/0310219.
- [33] G. Isidori, D. Lancerini, S. Nabeebaccus, and R. Zwicky, (2022), arXiv:2205.08635 [hep-ph].
- [34] R. Aaij *et al.* (LHCb), *Phys. Rev. Lett.* **113**, 151601 (2014), arXiv:1406.6482 [hep-ex].
- [35] R. Aaij *et al.* (LHCb), *Phys. Rev. Lett.* **122**, 191801 (2019), arXiv:1903.09252 [hep-ex].
- [36] R. Aaij *et al.* (LHCb), *Nature Phys.* **18**, 277 (2022), arXiv:2103.11769 [hep-ex].
- [37] R. Aaij *et al.* (LHCb), *JHEP* **08**, 055 (2017), arXiv:1705.05802 [hep-ex].
- [38] R. Aaij *et al.* (LHCb), *Phys. Rev. Lett.* **128**, 191802 (2022), arXiv:2110.09501 [hep-ex].
- [39] G. D'Ambrosio, A. M. Iyer, F. Mahmoudi, and S. Neshatpour, (2022), arXiv:2206.14748 [hep-ph].
- [40] M. Aaboud *et al.* (ATLAS), *JHEP* **04**, 098 (2019), arXiv:1812.03017 [hep-ex].
- [41] A. M. Sirunyan *et al.* (CMS), *JHEP* **04**, 188 (2020), arXiv:1910.12127 [hep-ex].
- [42] R. Aaij *et al.* (LHCb), *Phys. Rev. D* **105**, 012010 (2022), arXiv:2108.09283 [hep-ex].
- [43] R. Aaij *et al.* (LHCb), *Phys. Rev. Lett.* **128**, 041801 (2022), arXiv:2108.09284 [hep-ex].
- [44] T. Hurth, F. Mahmoudi, D. M. Santos, and S. Neshatpour, *Phys. Lett. B* **824**, 136838 (2022), arXiv:2104.10058 [hep-ph].
- [45] M. Algueró, B. Capdevila, S. Descotes-Genon, J. Matias, and M. Novoa-Brunet, *Eur. Phys. J. C* **82**, 326 (2022), arXiv:2104.08921 [hep-ph].
- [46] W. Altmannshofer and P. Stangl, *Eur. Phys. J. C* **81**, 952 (2021), arXiv:2103.13370 [hep-ph].
- [47] M. Ciuchini, M. Fedele, E. Franco, A. Paul, L. Silvestrini, and M. Valli, *Phys. Rev. D* **103**, 015030 (2021), arXiv:2011.01212 [hep-ph].
- [48] L.-S. Geng, B. Grinstein, S. Jäger, S.-Y. Li, J. Martin Camalich, and R.-X. Shi, *Phys. Rev. D* **104**, 035029 (2021), arXiv:2103.12738 [hep-ph].
- [49] D. London and J. Matias, (2021), 10.1146/annurev-nucl-102020-090209, arXiv:2110.13270 [hep-ph].
- [50] S. Jäger and J. Martin Camalich, *Phys. Rev. D* **93**, 014028 (2016), arXiv:1412.3183 [hep-ph].
- [51] T. Hurth, F. Mahmoudi, and S. Neshatpour, *Phys. Rev. D* **102**, 055001 (2020), arXiv:2006.04213 [hep-ph].
- [52] V. G. Chobanova, T. Hurth, F. Mahmoudi, D. Martinez Santos, and S. Neshatpour, *JHEP* **07**, 025 (2017), arXiv:1702.02234 [hep-ph].
- [53] S. S. Wilks, *Annals Math. Statist.* **9**, 60 (1938).
- [54] A. Arbey, T. Hurth, F. Mahmoudi, and S. Neshatpour, *Phys. Rev. D* **98**, 095027 (2018), arXiv:1806.02791 [hep-ph].
- [55] F. Mahmoudi, *Comput. Phys. Commun.* **178**, 745 (2008), arXiv:0710.2067 [hep-ph].
- [56] F. Mahmoudi, *Comput. Phys. Commun.* **180**, 1579 (2009), arXiv:0808.3144 [hep-ph].
- [57] F. Mahmoudi, *Comput. Phys. Commun.* **180**, 1718 (2009).
- [58] S. Neshatpour and F. Mahmoudi, *PoS TOOLS2020*, 036 (2021), arXiv:2105.03428 [hep-ph].
- [59] S. Neshatpour and F. Mahmoudi, *PoS CompTools2021*, 010 (2022), arXiv:2207.04956 [hep-ph].
- [60] S. Choudhury *et al.* (BELLE), *JHEP* **03**, 105 (2021), arXiv:1908.01848 [hep-ex].
- [61] A. M. Sirunyan *et al.* (CMS), *Phys. Rev. D* **98**, 112011 (2018), arXiv:1806.00636 [hep-ex].
- [62] R. Aaij *et al.* (LHCb), *JHEP* **12**, 081 (2020), arXiv:2010.06011 [hep-ex].
- [63] “Flavour Anomalies Workshop - Implications of LHCb Measurements and Future Prospects,” <https://indico.cern.ch/event/1055780> (CERN, October 19-22, 2021).
- [64] “Beyond the flavour anomalies III workshop,” <https://conference.ipp.dur.ac.uk/event/1064/> (Durham, Apr 26 – 28, 2022).
- [65] J. Bhom, M. Chrzaszcz, F. Mahmoudi, M. T. Prim, P. Scott, and M. White, *Eur. Phys. J. C* **81**, 1076 (2021), arXiv:2006.03489 [hep-ph].
- [66] A. K. Alok, A. Dighe, S. Gangal, and D. Kumar, *JHEP* **06**, 089 (2019), arXiv:1903.09617 [hep-ph].
- [67] A. Datta, J. Kumar, and D. London, *Phys. Lett. B* **797**, 134858 (2019), arXiv:1903.10086 [hep-ph].
- [68] K. Kowalska, D. Kumar, and E. M. Sessolo, *Eur. Phys. J. C* **79**, 840 (2019), arXiv:1903.10932 [hep-ph].
- [69] R. Aaij *et al.* (LHCb), *Expression of Interest for a Phase-II LHCb Upgrade*, Tech. Rep. (CERN, 2017).